

# Photo- and Electro-excitation of Bound Neutrons and Protons

Satoshi X. Nakamura

Received: date / Accepted: date

**Abstract** Data for pion photo-productions off the neutron ( $\gamma n \rightarrow \pi N$ ) have been primarily extracted from deuteron-target data ( $\gamma d \rightarrow \pi NN$ ) by applying kinematical cuts thereby isolating the quasi-free samples. We critically examine if the neutron-target data obtained through this conventional procedure can be contaminated by final state interactions (FSI) and/or the kinematical cuts. The analysis is conducted with a theoretical model for  $\gamma d \rightarrow \pi NN$  that takes account of the impulse mechanisms supplemented by the  $NN$  and  $\pi N$  rescattering mechanisms. We show that the FSI effects still visibly remain in the extracted  $\gamma' n' \rightarrow \pi N$  unpolarized cross sections and polarization asymmetries  $E$  even after the kinematical cuts are applied. We also find the FSI effects on  $\gamma' n' \rightarrow \pi^0 n$  can be somewhat different from those on  $\gamma' p' \rightarrow \pi^0 p$ .

## 1 Introduction

Meson production experiments with photon and electron beams have been very active at facilities worldwide. A main interest is to gain information on the properties of nucleon resonances ( $N^*$ ) such as their pole positions and electromagnetic transition form factors, using data complementary to those from the  $\pi N$  scattering. Even the so-called over-complete measurement is planned to accurately determine the amplitudes and thus  $N^*$  properties with significantly reduced model-dependence. Lots of achievements towards this direction have been made, particularly with the free-proton target experiments, and are summarized in this workshop [1].

To gain a complete picture of the  $N^*$  properties, we need not only proton-target data but also neutron-target data. Measurements of the neutron-target

---

S.X. Nakamura  
Laboratório de Física Teórica e Computacional-LFTC, Universidade Cruzeiro do Sul  
São Paulo, SP, 01506-000, Brazil  
E-mail: sxnakamura@gmail.com

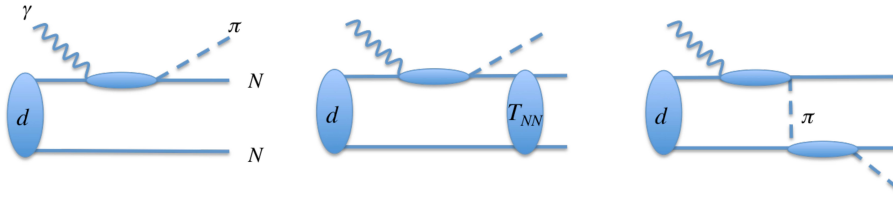


**Fig. 1** Diagrammatic representation of reaction mechanisms considered in this work for  $\gamma d \rightarrow \pi NN$ : (left) impulse, (center)  $NN$  rescattering, (right)  $\pi N$  rescattering mechanisms.

data, including polarization observables, have been also active recently. For example, unpolarized differential cross sections ( $d\sigma/d\Omega_\pi$ ) and the polarization observable  $E$  for  $\gamma n \rightarrow \pi^0 n$  have been measured at the MAMI [2,3], those for  $\gamma n \rightarrow \pi^- p$  at the JLab [4,5], and those for  $\gamma n \rightarrow \eta n$  at the MAMI [6,7,8]. More new (preliminary) results have been presented in this workshop [9].

The primary interest in the neutron-target data is the electromagnetic neutron-to- $N^*$  transition form factors. These  $\gamma^{(*)}n \rightarrow N^*$  form factors are combined with the  $\gamma^{(*)}p \rightarrow N^*$  form factors to give the isospin structure of the  $\gamma^{(*)}N \rightarrow N^*$  form factors that are interesting quantities for understanding the hadron structures. The isospin decomposition is also necessary when we apply the form factors to calculations of neutrino-induced meson productions [10]. In addition to these primary interests, the actual data have also brought unexpected surprises;  $\gamma n \rightarrow \eta n$  cross section data [6,11,12] revealed a narrow peak at  $W \sim 1.68$  GeV ( $W$ : the meson-baryon invariant mass) which had not been found in the  $\pi N$  and  $\gamma p$  reaction data.

The deuteron has been primarily used in the experiments to extract the neutron-target data. Conventionally, a certain set of kinematical cuts is applied to the deuteron data to supposedly isolate the quasi-free samples. However, this procedure has been always with a concern that the kinematical cuts and/or nuclear effects such as final state interactions (FSI) could distort the extracted neutron data from the true free neutron-target observables. The purpose of this work is to critically examine within a theoretical model the effects of the FSI and kinematical cuts on (un)polarized  $\gamma n \rightarrow \pi N$  cross sections extracted from  $\gamma d \rightarrow \pi NN$  cross sections.

## 2 Model

This study will be based on a  $\gamma d \rightarrow \pi NN$  reaction model that consists of the impulse [Fig. 1(left)],  $NN$  rescattering [Fig. 1(center)], and  $\pi N$  rescattering [Fig. 1(right)] mechanisms. The model needs to be incorporated with realistic elementary amplitudes for the subprocesses involved. Regarding  $\gamma N \rightarrow \pi N$  and  $\pi N \rightarrow \pi N$  amplitudes, we employ those generated with a dynamical coupled-channels (DCC) model [13,14]. The DCC model takes account of coupled-channels relevant to the nucleon resonance region, and has been developed through analyzing  $\sim 27,000$  data points of  $\pi N$ ,  $\gamma N \rightarrow \pi N$ ,  $\eta N$ ,  $K\Lambda$ ,  $K\Sigma$

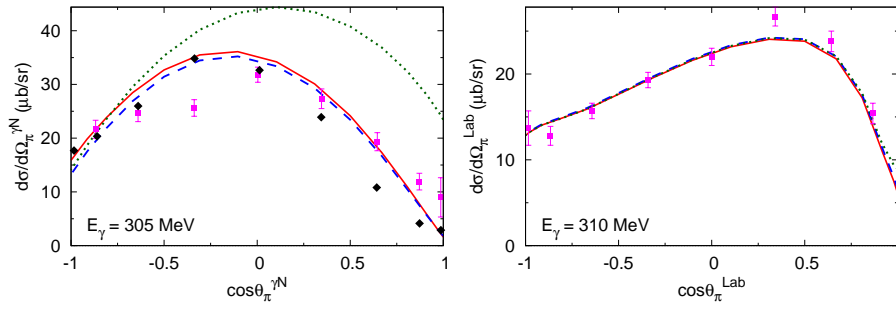


**Fig. 2** The pion angular distribution for  $\gamma d \rightarrow \pi^0 p n$  (left) and  $\gamma d \rightarrow \pi^- p p$  (right). The photon energy in the laboratory frame is indicated in the figure. The curves are obtained with the impulse approximation (green dotted), the impulse and  $NN$  rescattering mechanisms (blue dashed), and the full model (red solid) that also includes the  $\pi N$  rescattering mechanism. The data are from Ref. [17] (magenta squares) and Ref. [18] (black diamonds) for  $\gamma d \rightarrow \pi^0 p n$ , and from Ref. [19] for  $\gamma d \rightarrow \pi^- p p$ .

from the thresholds up to  $W \lesssim 2.1$  GeV. As for the deuteron wave function and the  $NN \rightarrow NN$  amplitudes, we employ those generated with the CD-Bonn potential [15].

### 3 Results (all numerical results are preliminary)

First we confront parameter-free model predictions for  $\gamma d \rightarrow \pi NN$  cross sections with data to examine the soundness of the model and FSI effects. Here, 'parameter-free' means that we did not adjust any model parameters using  $\gamma d \rightarrow \pi NN$  cross section data. The comparisons are presented in Fig. 2. The agreement with data is reasonably good overall. For  $\gamma d \rightarrow \pi^0 p n$ , a large reduction of the cross sections due to the  $NN$  rescattering is essential for the good agreement with the data. This reduction is mainly caused by the orthogonality between the deuteron wave function and the  ${}^3S_1$  partial wave in the final  $NN$  state. The  $\pi N$  rescattering effect is rather moderate. Meanwhile, for  $\gamma d \rightarrow \pi^- p p$  where the orthogonality mentioned above does not come into play, the FSI effects are rather small. We mention that the DCC-based deuteron reaction model predicts  $\gamma d \rightarrow \eta p n$  cross sections that are in excellent agreement with data [16].

We also present in Fig. 3 the polarization asymmetry  $E$  defined by  $E = (\sigma_{+-} - \sigma_{++}) / (\sigma_{+-} + \sigma_{++})$ , where  $\sigma_{++}$  ( $\sigma_{+-}$ ) is the  $\gamma d \rightarrow \pi NN$  cross section for which the photon circular polarization and the deuteron spin orientation are parallel (antiparallel). Comparing Figs. 2 and 3, we find that the FSI effects on the  $\gamma d \rightarrow \pi^0 p n$  cross sections are significantly canceled in the ratio  $E$ .

Now we extract cross sections (including polarization observables) for quasi-free  $\gamma n \rightarrow \pi N$  from those for  $\gamma d \rightarrow \pi NN$  in a conventional manner. A set of kinematical cuts is applied to the  $\gamma d \rightarrow \pi NN$  cross sections generated with the DCC-based model, and then further correction is made for the Fermi mo-

	$d\sigma/d\Omega_\pi$ [5]	$E$ [4]
$\pi^-$ momentum (GeV)	$> 0.1$	$> 0.4$
Faster proton momentum (GeV)	$> 0.36$	$> 0.4$
Slower proton momentum (GeV)	$< 0.2$	$< 0.1$
$\Delta\phi =  \phi_{\pi^-} - \phi_{\text{faster proton}} $	-	$160^\circ < \Delta\phi < 200^\circ$

**Table 1** The kinematical cuts used in the experimental analyses [4,5] for extracting unpolarized cross sections ( $d\sigma/d\Omega_\pi$ ) and the polarization asymmetry  $E$  for  $\gamma n \rightarrow \pi^- p$  from those for  $\gamma d \rightarrow \pi^- pp$ . The azimuthal angle difference between  $\pi^-$  and the faster proton is denoted by  $\Delta\phi$ .

tion (Fermi-unsmearing). By comparing the extracted quasi-free cross sections with the corresponding free ones, which are calculated with the same elementary amplitudes used in the  $\gamma d \rightarrow \pi NN$  model, we address the questions on how the extracted cross sections could be distorted by the FSI and kinematical cuts. We employ the kinematical cuts that have been used in recent experimental analyses to extract  $\gamma n \rightarrow \pi^- p$  from  $\gamma d \rightarrow \pi^- pp$ , as summarized in Table 1. We also use the same cuts to extract  $\gamma n \rightarrow \pi^0 n$  from  $\gamma d \rightarrow \pi^0 pn$ . For the Fermi-unsmearing, we follow the procedure described in Appendix B of Ref. [20].

We show in Fig. 4 the quasi-free  $\gamma n \rightarrow \pi^0 n$  cross sections extracted from theoretical  $\gamma d \rightarrow \pi^0 pn$  cross section, using the kinematical cuts of Table 1 and the Fermi unsmearing. The green triangles (blue circles) [red squares] in the figure are extracted from the  $\gamma d \rightarrow \pi^0 pn$  cross sections calculated with the impulse approximation (the impulse and  $NN$  rescattering mechanisms) [the full model]. The phase-space integral has been done with the Monte-Carlo method, and thus the numerical results are given by the points with error bars; the errors include only statistical ones associated with the Monte-Carlo method. The kinematical cuts remove the forward  $\pi$  kinematical regions. We can see that a significant reduction due to the FSI remains even after the kinematical cuts have been applied. The  $NN$  and  $\pi N$  FSI contributions are comparably visible. Therefore, only the quasi-free cross sections extracted from

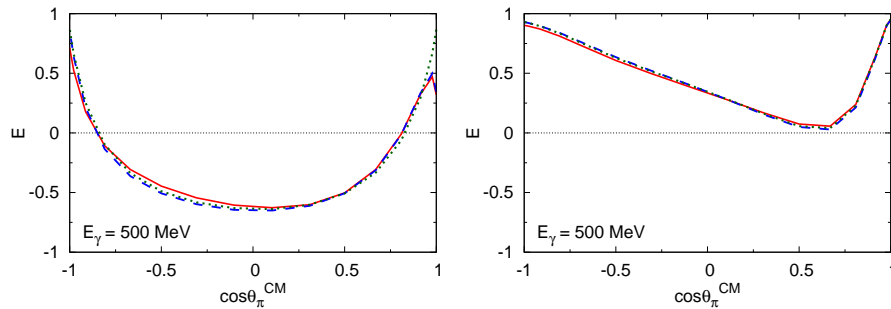


**Fig. 3** The polarization asymmetry  $E$  for  $\gamma d \rightarrow \pi^0 pn$  (left) and  $\gamma d \rightarrow \pi^- pp$  (right). The other features are the same as those in Fig. 2.

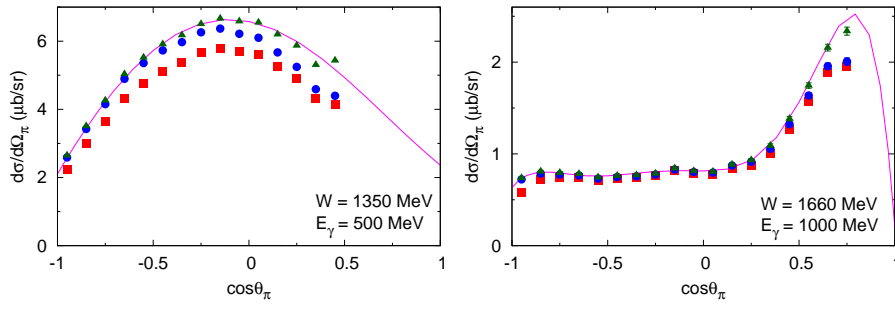


**Fig. 4** The pion angular distribution for  $\gamma n \rightarrow \pi^0 n$  extracted from  $\gamma d \rightarrow \pi^0 pn$ . The photon energy ( $E_\gamma$ ) in the laboratory frame and the final  $\pi^0 n$  invariant mass ( $W$ ) for  $\gamma d \rightarrow \pi^0 pn$  are indicated in the figure. The points with error bars are extracted from theoretical  $\gamma d \rightarrow \pi^0 pn$  differential cross sections, using the kinematical cuts of Table 1 and the Fermi unsmearing. When the theoretical  $\gamma d \rightarrow \pi^0 pn$  cross sections are calculated with the impulse approximation (the impulse and  $NN$  rescattering mechanisms) [the full model], the green triangles (blue circles) [red squares] are obtained. The errors are only statistical from the Monte-Carlo integral, and are not shown when smaller than the point size. The solid curve is the free  $\gamma n \rightarrow \pi^0 n$  cross sections at  $W$  from the DCC model.

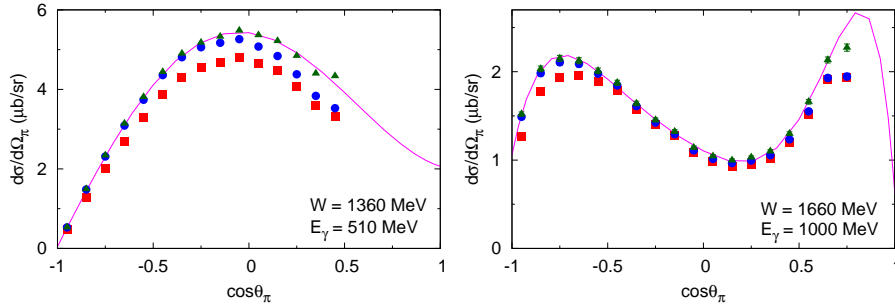


**Fig. 5** The pion angular distribution for  $\gamma p \rightarrow \pi^0 p$  extracted from  $\gamma d \rightarrow \pi^0 pn$ . The other features are the same as those in Fig. 4.

$\gamma d \rightarrow \pi^0 pn$  calculated with the impulse approximation reproduce well the free cross sections.

It would be interesting to compare the FSI effects on the quasi-free  $\gamma n \rightarrow \pi^0 n$  and those on the  $\gamma p \rightarrow \pi^0 p$  cross sections. This is particularly important because an experimental analysis sometimes assumes that the FSI effects are the same for both, as in Ref. [2]. Therefore, we show in Fig. 5 the quasi-free  $\gamma p \rightarrow \pi^0 p$  cross sections. By comparing Figs. 4 and 5, the FSI effects are somewhat different between  $\gamma n \rightarrow \pi^0 n$  and  $\gamma p \rightarrow \pi^0 p$  cross sections; generally a few percents difference in the reduction rates.

Next we discuss the polarization observable  $E$  for the quasi-free  $\gamma n \rightarrow \pi^0 n$ . This polarization asymmetry is defined by  $E = (\sigma_{1/2} - \sigma_{3/2}) / (\sigma_{1/2} + \sigma_{3/2})$ , where  $\sigma_{3/2}$  ( $\sigma_{1/2}$ ) is the  $\gamma N$  cross section for which the photon circular

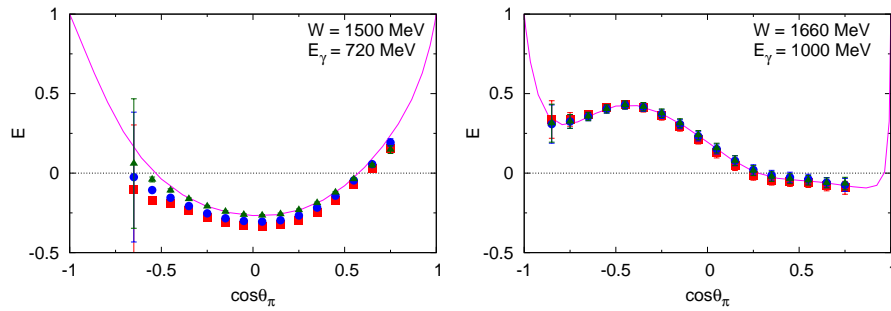


**Fig. 6** The polarization observable  $E$  for  $\gamma n \rightarrow \pi^0 n$  extracted from  $\gamma d \rightarrow \pi^0 pn$ . The other features are the same as those in Fig. 4.

polarization and the nucleon spin orientation are parallel (antiparallel). We show in Fig. 6  $E$  for the quasi-free  $\gamma n \rightarrow \pi^0 n$ . The magnitude of the FSI effects on  $E$  are smaller than those on  $d\sigma/d\Omega_\pi$  because of the partial cancellation in the ratio. The previous experimental analysis [3] assumed no FSI effects on  $E$ , invoking the cancellation. However, we can still see nonnegligible FSI effects on  $E$  for  $\gamma n \rightarrow \pi^0 n$  at some  $W$ , and thus depending on the precision of data, corrections from this effect would be needed.

Finally, we study the FSI effects on  $d\sigma/d\Omega_\pi$  and  $E$  for the quasi-free  $\gamma n \rightarrow \pi^- p$  extracted from  $\gamma d \rightarrow \pi^- pp$ . Our numerical result is give in Fig. 7. We again find that the quasi-free cross sections extracted from  $\gamma d \rightarrow \pi^- pp$  in the impulse approximation reproduce well the free cross sections. For the backward pion kinematics, we find  $\sim 9\%$  reduction of  $d\sigma/d\Omega_\pi$  at  $W = 1500$  MeV due to the  $\pi N$  rescattering. Tarasov et al. also reported a similar finding [21]. Regarding the polarization asymmetry  $E$ , we do not find a visible FSI effect. However, we find that the extracted quasi-free  $E$  at the kinematical ends are noticeably different from the free  $E$ . This might be an artifact of the kinematical cuts, and a more elaborate study is underway.

As seen in Figs. 4-7, the FSI effects often shift the extracted  $\gamma n \rightarrow \pi N$  observables from the corresponding free ones. This may seem to indicate that we cannot correctly extract  $\gamma n \rightarrow \pi N$  observables using the conventional method based on the kinematical cuts. Meanwhile, it is not computationally practical to determine the  $\gamma n \rightarrow \pi N$  amplitudes (and thus the observables) by directly fitting them to the  $\gamma d \rightarrow \pi NN$  data through a reaction model such as the one used in this work. A possible option would be to take an iterative procedure as follows:

1. Start with a certain set of parameters of a dynamical model that generates  $\gamma n \rightarrow \pi N$  amplitudes. Implement the amplitudes into a dynamical  $\gamma d \rightarrow \pi NN$  reaction model.
2. With the same set of kinematical cuts as used in an experiment, calculate  $\gamma d \rightarrow \pi NN$  cross sections with the dynamical model including the FSI, and extract the  $\gamma n \rightarrow \pi N$  cross sections using the conventional method.

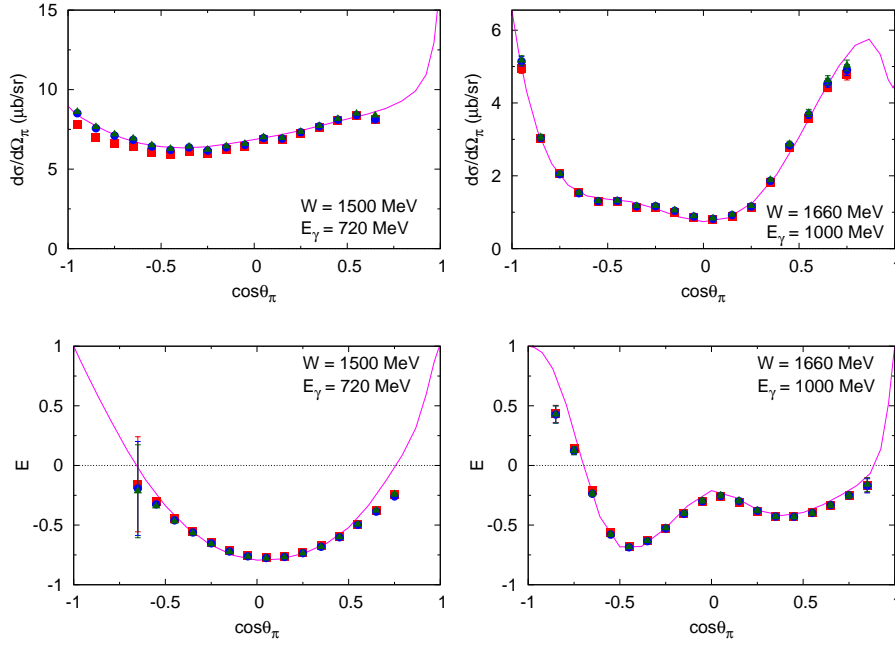


**Fig. 7** The  $d\sigma/d\Omega_\pi$  and  $E$  for  $\gamma n \rightarrow \pi^- p$  extracted from  $\gamma d \rightarrow \pi^- pp$ . The other features are the same as those in Fig. 4.

By comparing the extracted  $\gamma n \rightarrow \pi N$  cross sections with the free ones from the  $\gamma n \rightarrow \pi N$  amplitudes built in the  $\gamma d$  model, the FSI correction factor on the extracted cross sections is obtained.

3. Extract  $\gamma n \rightarrow \pi N$  data from  $\gamma d \rightarrow \pi NN$  experimental data using the conventional method. The obtained quantity is further multiplied by the FSI correction factor estimated in the previous step, then  $\gamma n \rightarrow \pi N$  cross section data are extracted.
4. Calculate  $\gamma n \rightarrow \pi N$  cross sections with the elementary amplitudes that have been built in the  $\gamma d$  model, and compare them with the extracted data. If they agree, the extraction of the  $\gamma n \rightarrow \pi N$  data as well as that of the corresponding amplitude are complete. If not, fit the extracted data with the dynamical model for  $\gamma n \rightarrow \pi N$  by adjusting their parameters, then return to the step 1.

**Acknowledgements** The author acknowledges H. Kamano, T.-S.H. Lee and T. Sato for their collaborations. This work was supported in part by Fundação de Amparo à Pesquisa do Estado de São Paulo-FAPESP, Process No. 2016/15618-8. Numerical computations in this work were carried out with SR16000 at YITP in Kyoto University, the High Performance Computing system at RCNP in Osaka University, the National Energy Research Scientific Computing Center, which is supported by the Office of Science of the U.S. Department of Energy under Contract No. DE-AC02-05CH11231, and resources provided on Blues and/or

Bebop, high-performance computing cluster operated by the Laboratory Computing Resource Center at Argonne National Laboratory.

## References

1. V.D. Burkert,  $N^*$  Experiments and their Impact on Strong QCD Physics. arXiv:1801.10480 (This proceedings)
2. A2 Collaboration, M. Dieterle, et al., Photoproduction of  $\pi^0$  Mesons off Neutrons in the Nucleon Resonance Region. Phys. Rev. Lett. **112**, 142001 (2014)
3. M. Dieterle, et al., First measurement of the polarization observable  $E$  and helicity-dependent cross sections in single  $\pi^0$  photoproduction from quasi-free nucleons. Phys. Lett. **B770**, 523 (2017)
4. CLAS Collaboration, D. Ho, et al., Beam-Target Helicity Asymmetry for  $\vec{\gamma} \vec{n} \rightarrow \pi^- p$  in the  $N^*$  Resonance Region. Phys. Rev. Lett. **118**, 242002 (2017)
5. CLAS Collaboration, P.T. Mattione, et al., Differential cross section measurements for  $\gamma n \rightarrow \pi^- p$  above the first nucleon resonance region. Phys. Rev. C **96**, 035204 (2017)
6. A2 Collaboration, D. Werthmüller, et al., Narrow Structure in the Excitation Function of  $\eta$  Photoproduction off the Neutron. Phys. Rev. Lett. **111**, 232001 (2013)
7. A2 Collaboration, D. Werthmüller, et al., Quasifree photoproduction of  $\eta$  mesons off protons and neutrons. Phys. Rev. C **90**, 015205 (2014)
8. A2 Collaboration, L. Witthauer, et al., Helicity-dependent cross sections and double-polarization observable  $E$  in  $\eta$  photoproduction from quasifree protons and neutrons. Phys. Rev. C **95**, 055201 (2017)
9. C. Gleason, this proceedings;  
H. Lu, this proceedings;  
Y. Tian, this proceedings;  
J. Zhang, this proceedings.
10. S.X. Nakamura, H. Kamano, T. Sato, Dynamical coupled-channels model for neutrino-induced meson productions in resonance region. Phys. Rev. D **92**, 074024 (2015)
11. V. Kuznetsov, et al., Evidence for a narrow structure at  $W \sim 1.68$  GeV in  $\eta$  photoproduction off the neutron. Phys. Lett. **B647**, 23 (2007)
12. The CBELSA/TAPS Collaboration, I. Jaegle, et al., Quasifree Photoproduction of  $\eta$  Mesons off the Neutron. Phys. Rev. Lett. **100**, 252002 (2008)
13. H. Kamano, S.X. Nakamura, T.-S. H. Lee, T. Sato, Nucleon resonances within a dynamical coupled-channels model of  $\pi N$  and  $\gamma N$  reactions. Phys. Rev. C **88**, 035209 (2013)
14. H. Kamano, S.X. Nakamura, T.-S. H. Lee, T. Sato, Isospin decomposition of  $\gamma N \rightarrow N^*$  transitions within a dynamical coupled-channels model. Phys. Rev. C **94**, 015201 (2016)
15. R. Machleidt, The High precision, charge dependent Bonn nucleon-nucleon potential. Phys. Rev. C **63**, 024001 (2001)
16. S.X. Nakamura, H. Kamano, T. Ishikawa, Low-energy  $\eta$ -nucleon interaction studied with  $\eta$  photoproduction off the deuteron. Phys. Rev. C **96**, 042201(R) (2017)
17. B. Krusche, et al., Single and double  $\pi^0$  photoproduction from the deuteron. Eur. Phys. J. **A6**, 309 (1999)
18. U. Siodlaczek et al., Coherent and incoherent  $\pi^0$  photoproduction from the deuteron. Eur. Phys. J. **A10**, 365 (2001)
19. Aachen-Bonn-Hamburg-Heidelberg-Muenchen Collaboration, P. Benz et al., Measurement of the reaction  $\gamma d \rightarrow \pi^- pp$ , and determination of cross-sections for the reaction  $\gamma n \rightarrow \pi^- p$ . at photon energies between 0.2-GeV and 2.0-GeV. Nucl. Phys. **B65**, 158 (1973)
20. V.E. Tarasov, W.J. Briscoe, M. Dieterle, B. Krusche, A.E. Kudryavtsev, M. Ostrick, I.I. Strakovsky, On the extraction of cross sections for  $\pi^0$  and  $\eta$  photoproduction off neutrons from deuteron data. Phys. Atom. Nucl. **79**, 216 (2016)
21. V.E. Tarasov, W.J. Briscoe, H. Gao, A.E. Kudryavtsev, I.I. Strakovsky, Extracting the photoproduction cross section off the neutron  $\gamma n \rightarrow \pi^- p$  from deuteron data with FSI effects. Phys. Rev. C **84**, 035203 (2011)